

Angular-Correlation Studies of Positron Annihilation in Copper-Nickel Alloys

Lawrence J. Rouse and Paul G. Varlashkin

Department of Physics and Astronomy, Louisiana State University, Baton Rouge, Louisiana 70803

(Received 25 March 1971)

Rectangular-slit detector geometry has been used to study the Fermi surface of three concentrations of nickel in copper. Measurements were made in the $\langle 111 \rangle$ and $\langle 110 \rangle$ directions on single crystals of the alloys with concentrations of 10, 50, and 90 at.% nickel. The belly radius of the Fermi surface is seen to decrease as the amount of nickel is increased. The radius of the necks in the $\langle 111 \rangle$ direction, however, does not appear to change substantially with change in alloy concentration. These necks are easily detected at concentrations of 10 and 50 at.% nickel and are still visible in the 90 at.% nickel alloy.

I. INTRODUCTION

Much work has been done on copper and its dilute alloys using conventional solid-state techniques.¹⁻⁴ Because of this the Fermi surface of copper is well known. These studies have shown that the Fermi surface has necks that reach out to the hexagonal-zone faces (the $\langle 111 \rangle$ directions). Much attention has been given to the study of the size of these necks in various dilute alloys of copper. These studies were restricted to very low concentrations of the solute material because of the shortening of the electron mean free path as the solute concentration is increased. The technique of positron annihilation allows the extension to all alloy concentrations since it is not restricted in this manner.

The original method of measurement of the angular correlation of radiation from positron annihilation employed long slits.⁵ This method enables an experimenter to measure the cross-sectional area of the Fermi surface, and consequently it is not very sensitive to the fine structure of the surface. Other methods which have used positron annihilation to study the electron momentum distribution of metals are the collinear-point detector geometry⁶ and the crossed-slit (rectangular-aperture) geometry.⁷ These two methods are able to reveal additional structure of the Fermi surface. A problem with the latter two methods is that because the detection slits subtend a small solid angle, the number of coincidences is reduced and the statistics of the measurements decreased. This problem is alleviated by the use of Cu⁶⁴ as the source of positrons. After irradiation by thermal neutrons the sample itself becomes the source and very efficient use is made of the positrons generated. All three methods have been previously used to measure the Fermi surface of copper and its alloys.⁶⁻⁸

We report here on rectangular-slit-type measurements of copper-nickel alloys in the compositions 90/10, 50/50, and 10/90.⁹ This is the first

report on the higher nickel concentrations.

II. THEORY

The two-photon angular-distribution function measured by the conventional long-slit geometry is given by

$$N(p_x) \propto \int \int_{-\infty}^{\infty} \rho(\vec{p}) dp_x dp_y,$$

where $\rho(\vec{p})$ is the probability that the annihilation photons have a total momentum \vec{p} . The coincidence counting rate in this case is a measure of the momentum distribution over slices in momentum space as specified by a particular magnitude and direction of \vec{p}_x . The normal procedure is to set up a model of the Fermi surface and attempt to fit the observations to it.

In our measurements an additional direction is restricted so that the angular-distribution function becomes

$$N(p_x, p_z) \propto \int_{-\infty}^{\infty} \rho(\vec{p}) dp_y.$$

By this method we fix p_x at zero and vary p_z so that we get the integral over a line of constant p_x and p_z through the Fermi surface. Our coincidence counting rate is a measure of a cross section of the momentum distribution. In principle from point-detector geometry a detailed and direct view of the Fermi surface may be obtained. In practice the measurement is complicated by a large fraction of the positrons annihilating with M -shell electrons, and by the fact that the finite size of the slits allows coincidences to be recorded over a small range of angles so that the annihilating electrons come from a rectangular volume through the Fermi surface.

III. EXPERIMENTAL TECHNIQUE

Our experimental arrangement was a variation of the crossed-slit geometry reported by Fujiwara and Sueoka (FS).⁷ The alloy crystal was placed midway between scintillation detectors spaced 500 in. apart. Instead of using one slit at each detector, two horizontal symmetrically spaced slits were placed at each end. The arrangement is sketched

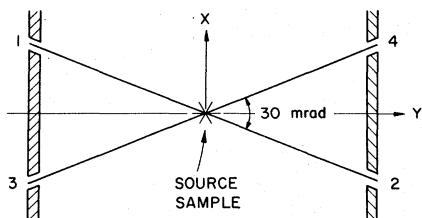


FIG. 1. Experimental slit arrangement. The distance from the source to the slits is 250 in. and the slits are 7 in. apart.

in Fig. 1. Slits 1 and 2 act as a rectangular-aperture system integrating in the 1-2 direction, and slits 3 and 4 as a rectangular-aperture detector system integrating in the 3-4 direction. The angular separation of adjacent slits (center to center) is 30 mrad or 1.72° . Since the 1-2 and 3-4 directions deviate from the y direction by only 0.86° and the angular width of the neck in copper is about 20° , each pair of slits may be considered to integrate in the y direction. However, in order for photons from any given annihilation to simultaneously enter slits 1 and 4 or 2 and 3, the angle between annihilation photons would have to differ from 180° by 30 mrad or more. Photon pairs whose directions differ from 180° by 30 mrad have a momentum of about five times the Fermi momentum.¹⁰ It is very unlikely that an annihilating electron in a metal will have five times the Fermi momentum and hence it is very improbable that the photon directions will differ from 180° by 30 mrad. The obvious advantage of this type of system over that of FS is that double the counting rate is obtained. The angle between annihilation photons was varied by moving one pair of detectors (1-3 or 2-4) vertically (in the z direction).

The detector slits were 0.5 in. wide in the 1-3 or 4-2 direction and 0.2 in. high in the vertical direction. Hence the geometrical resolution functions associated with the slits are 2.0 and 0.8 mrad full width at half-maximum (FWHM). Because alignment is very critical in rectangular-slit geometry, after initial alignment the detectors were removed from behind the slits and a small laser used for final adjustments.

Our crystals were rectangular parallelepipeds with dimensions of $0.25 \times 0.25 \times 0.1$ in. In all cases the large face was horizontal and one of the small crystal faces was perpendicular to the y direction. The relative orientations of the crystals and the geometrical resolution functions were the same as those of FS. The Cu-Ni crystals were mounted on a polycrystalline copper pedestal. Some of the positrons produced close to the surface escaped from the crystal and annihilated in the pedestal. Since the mean range of positrons from Cu^{64} is only about 30 mg/cm^2 , the contribution from

positrons annihilating in the pedestal will be negligibly small.

In the type of measurement where the target is itself the source of positrons, the dimensions of the source sample must be taken into account in calculating the total geometrical resolution of the system. If one considers the crystal to be made up of many thin layers and adds up the contributions from each layer, the resultant over-all instrumental angular resolution functions are approximately 1.0 and 2.6 mrad FWHM for the vertical and horizontal resolution functions, respectively. FS report resolution functions of 0.85 and 5.5 mrad FWHM for their narrow and broad resolution functions. Hence, although our narrow resolution function is not quite as good, the broad resolution function is twice as sharp. We therefore expect to be able to see more of the fine structure and to be less subject to some of the criticisms previously applied to our type of system.⁸

The crystals (fabricated by Ventron Electronics) were irradiated for 24 h in the Georgia Tech Research reactor in a thermal-neutron flux of about 1.5×10^{13} neutrons/cm² sec. This irradiation produced Cu^{64} activities of approximately 7, 4, and 1 Ci for the 90/10, 50/50, and 10/90 Cu-Ni ratios, respectively. Because of the short half-life of Cu^{64} (12.8 h), the crystals were flown to us from the reactor and were placed in the angular-correlation apparatus about $6\frac{1}{2}$ -7 h after being removed from the reactor. Initial side-channel (noncoincidence) counting rates ranged as high as 8000 counts/sec. The coincidence circuit was operated with a resolution time of $\tau = 30$ nsec. At the start of each data run the accidental-coincidence counting rate was measured and this background (suitably corrected for the decay of Cu^{64}) subtracted from the coincidence counts recorded at each data point. Some of the crystals were irradiated several times in order to check reproducibility of the angular-correlation curves. These crystals were checked for structural damage by backscattering of x rays. No effect of radiation was visible in the resultant Laue patterns.

The crystals were also checked for impurity production during the irradiation with a γ -ray spectrometer. Tests showed only very minute impurities, notably Ag^{110m} and Au^{198} .

IV. RESULTS

The angular-correlation curves for each alloy show the data for the following orientations: (a) For the samples marked $\langle 111 \rangle$, the direction of the radiation is parallel to $[111]$ and the component of the momentum is parallel to $[\bar{1}10]$, and (b) for the samples marked $\langle 110 \rangle$, the direction of the radiation

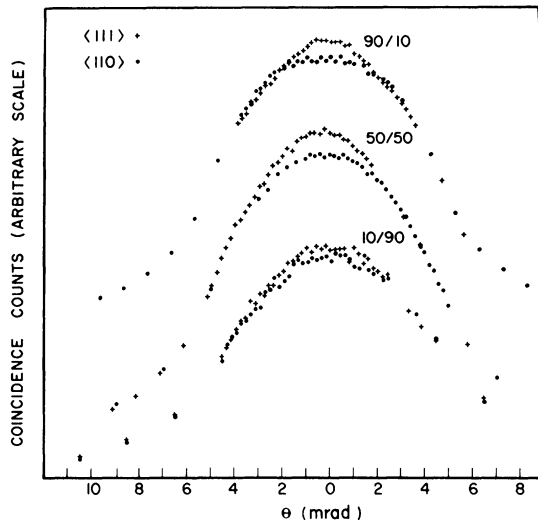


FIG. 2. Angular-correlation curves for positrons annihilating in two orientations and three copper-nickel alloy concentrations.

is parallel to $[1\bar{1}0]$ and the component of the momentum is parallel to $[111]$.

The data for the three concentrations are shown in Fig. 2. The raw data have been corrected for the decay of the source and the accidental background has been subtracted. The distributions for both directions, $\langle 111 \rangle$ and $\langle 110 \rangle$, are shown normalized to the same value at one-half the Fermi momentum. In all three alloys we are able to detect a difference between the two orientations near $\theta = 0$.

The high-angle tail is attributed to annihilation with M -shell electrons, possibly enhanced by higher-momentum components of electrons Bragg reflected into the second zone. The effect of these annihilations can be largely removed by subtracting a Gaussian fitted to the large-angle data.^{8,11}

The Fermi surface of copper is essentially a sphere with necks reaching out to contact the zone boundary in the $\langle 111 \rangle$ directions³ (see Fig. 3). The Fermi surface of nickel is similar to copper.¹² It therefore seems logical to assume that the Fermi

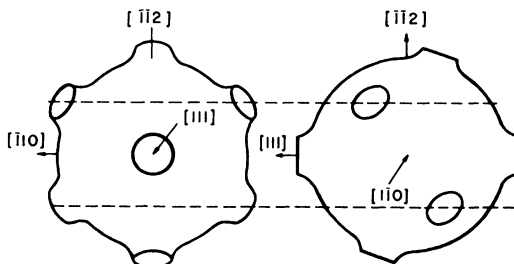


FIG. 3. Representation of the Fermi surface of pure copper.

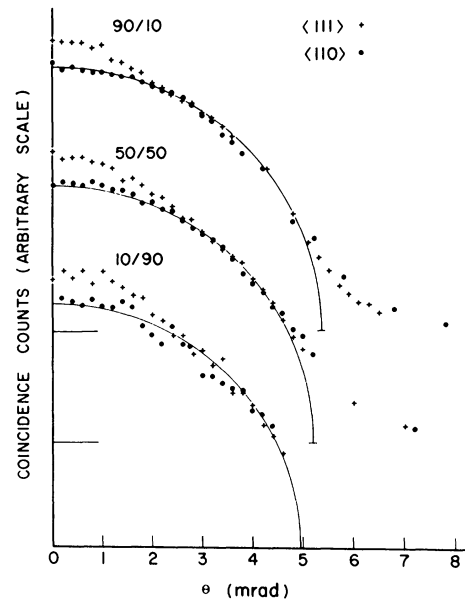


FIG. 4. Reduced data from Fig. 2. To account for annihilation with core electrons a Gaussian has been subtracted and the resulting difference curve has been adjusted in vertical scale to best fit a circle. The radii of the circles are given in Table I. Only one side of $\theta = 0$ is plotted.

surface of the alloys is similar in shape. The cross section is, hence, circular except in the vicinity of the necks.

The data, after subtracting the Gaussian representing the core annihilation, have been renormalized to best fit a circle. The results of this type of analysis are shown in Fig. 4. In all three alloys, the data points for the $\langle 111 \rangle$ sample depart from the circle near $\theta = 0$ (the $\langle 111 \rangle$ directions). The bump in the $\langle 111 \rangle$ direction is ascribed to the Fermi-surface necks. In the $\langle 110 \rangle$ direction the data fit the circle extremely well with the exception of 10/90 sample, where the scatter is attributed to poor statistics.

The radius of the neck of the Fermi surface of pure copper is about 1 mrad.⁷ If we examine the bumps ascribed to the Fermi-surface necks we find in all three alloys that the flat region near $\theta = 0$ extends to about 1 mrad before the data points begin to fall toward the circle (see Fig. 3). Although the apparatus resolution smears the data in the region of the neck we can still make some conclusions about the neck's size. If we assume that the neck of the Fermi surface of the 90/10 sample will have about the same radius as that for pure copper then, because all three alloys have similar shapes of the bumps ascribed to the necks, all three alloys can be said to show the same radius for the neck (about 1 mrad).

The belly radius is seen to change with the change

TABLE I. Experimentally determined parameters.

Alloy conc	Belly radius (mrad)	Neck radius (mrad)	Peak coincidence (counts/point)
90/10	5.35	1.0	42 000
50/50	5.2	1.0	30 000
10/90	4.95	1.0	5 700

in the relative concentration of the constituents. As the percentage of nickel increases, the belly radius decreases. This is to be expected from the fact that the number of conduction electrons is decreasing as nickel atoms are substituted for copper atoms. The values for various dimensions of the Fermi surface are shown in Table I.

The lack of a sharp discontinuity in the slope of the angular-correlation curves at the Fermi mo-

mentum has been observed by others in other metals. The smearing at the expected Fermi momentum has been variously attributed to breakdown of the free-electron behavior near the zone boundary,¹³ to a broadening of the wave number in an alloy,¹⁴ and to the existence of annihilations with high-momentum components due to conduction electrons in the second zone.¹¹ Our data do not give any new information on the cause of the smearing as we did not concentrate on the region around the Fermi momentum.

ACKNOWLEDGMENTS

This work was partially supported by a grant from the Research Corporation. The authors would like to thank Dr. E. F. Zganjar for useful discussions and the use of the γ -ray spectrometer, and also Dr. Joseph Callaway for useful discussions.

¹A. B. Pippard, Phil. Trans. Roy. Soc. London **A250**, 323 (1957).

²D. N. Langenberg and T. W. Moore, Phys. Rev. Letters **3**, 328 (1959).

³D. Shoenberg, in *The Fermi Surface*, edited by W. A. Harrison and M. B. Webb (Wiley, New York, 1960), p. 74.

⁴L. R. Chollet and I. M. Templeton, Phys. Rev. **170**, 656 (1968).

⁵S. DeBenedetti, C. E. Cowan, W. R. Konneker, and H. Primakoff, Phys. Rev. **77**, 205 (1950).

⁶D. L. Williams, E. H. Becker, P. Petijevich, and G. Jones, Phys. Rev. Letters **20**, 448 (1968).

⁷K. Fujiwara and O. Sueoka, J. Phys. Soc. Japan **21**,

1947 (1966).

⁸B. W. Murray and J. D. McGervey, Phys. Rev. Letters **24**, 9 (1970).

⁹We will adopt the convention A/B in referring to the copper-nickel alloys. A will be the atomic percentage of copper, and B will be that of nickel.

¹⁰1 mrad corresponds to 2.7308×10^{-20} g cm/sec.

¹¹S. Berko and J. S. Plaskett, Phys. Rev. **112**, 1877 (1958).

¹²H. Ehrenreich, H. R. Philipp, and D. J. Olechna, Phys. Rev. **131**, 2469 (1963).

¹³K. Fujiwara and O. Sueoka, J. Phys. Soc. Japan **23**, 1242 (1967).

¹⁴E. A. Stern, Phys. Rev. **168**, 730 (1968).

Magnetic Susceptibility of Alkali Metals*

A. Isihara and J. T. Tsai
*Statistical Physics Laboratory, Department of Physics and Astronomy,
 State University of New York, Buffalo, New York 14214*

(Received 14 June 1971)

The magnetic susceptibility of alkali metals is evaluated by a systematic development of the grand partition function for small magnetic fields. The results are expressed in powers of r_s (the interparticle spacing divided by the Bohr radius) and compared with recent experimental and theoretical results. The evaluation is made to order r_s^2 , improving the previous calculations. The polarization parameter, which has been used in the previous evaluation of the paramagnetic susceptibility as an adjustable parameter, is not used. Comparison of our results with the recent experiment by Collings is satisfactory.

I. INTRODUCTION

Recently we have considered the effects of Coulomb interactions on the diamagnetic susceptibility of an electron gas. We found at high temperatures a small increase in the susceptibility that is pro-

portional to the plasma parameter¹ and at low temperatures a much larger increase due to an exchange effect.² A similar increase in the diamagnetic susceptibility has been observed by March and Donovan and by Kanazawa and Matsudaira.³

In this paper we shall extend our previous consid-